Digest Journal of Nanomaterials and Biostructures Vol. 13, No. 1, January - March 2018, p. 285 - 297

SYNTHESIS AND CHARACTERIZATION OF UN-DOPED AND COPPER-DOPED ZINC OXIDE NANOPARTICLES FOR THEIR OPTICAL AND ANTIBACTERIAL STUDIES

S. A. KHAN[a*], S. SHAHID[a], S. JABIN[a], S. ZAMAN[b], M. N. SARWAR[b]
[a]*Department of Chemistry, School of Science, University of Management & Technology, Lahore-54770, Pakistan*
[b]*Ibn-e-Sina Institute of Technology, Islamabad-44000, Pakistan*

In the present study, synthesis, characterization and antibacterial properties of un-doped and Cu-doped ZnO nanoparticles (NAPs) were explored and also have been investigated the effect of changing the dopant precursor material [$Cu(NO_3)_2$ to $Cu(NO_3)_2.3H_2O$] on the surface morphology and the antibacterial properties of Cu-doped ZnO NAPs. The un-doped ZnO NAPs, Cu-doped ZnO NAPs (M1 NAPs, $Cu(NO_3)_2$) and (M2 NAPs, $Cu(NO_3)_2.3H_2O$) were fabricated through co-precipitation method. The synthesized NAPs were characterized by different spectroscopic and analytical techniques such as X-Ray Diffraction (XRD), scanning electron microscopy (SEM), energy-dispersive X-ray spectroscopy (EDAX) and Ultraviolet-visible (UV-Vis) spectroscopy. The antibacterial activity of synthesized NAPs was carried out by agar diffusion method against different bacterial strains. Results from XRD, SEM, EDAX and UV-Vis examines confirmed the successful synthesis, crystalline nature and hexagonal wurzite structure of un-doped and M1 NAPs and M2 NAPs with the average grain size of 15.63 nm and 20.18 nm and 28.94 nm; and band gap energy of 3.68, 2.76 eV and 2.10 eV respectively. The synthesized Cu-doped ZnO NAPs (M2 NAPs) were disclosed the remarkable and extraordinary antibacterial activity against *E. coli*, and *B. subtilis*, with the zone of inhibitions of 31 ± 0.4 mm and 27 ± 0.6 mm, respectively. Better and improved antibacterial propensity was also demonstrated by M1 NAPs than un-doped ZnO NAPs and standard drug. Results thus obtained corroborate and suggest the applications of un-doped ZnO NAPs and Cu-doped ZnO NAPs as antibacterial agents. Therefore, they are worthy candidates for future pharmaceutical applications.

(Received January 13, 2018; Accepted March 6, 2018)

Keywords: Synthesis, Cu-doped ZnO NAPs, characterization, optical, Antibacterial, activity

1. Introduction

Human beings are interfacing the range of diseases produced by different pathogenic microorganisms since prehistoric times [1,2]. Scientists are making an effort to design and develop various chemical species i.e. natural, biochemical, nanoparticles etc. to cope with these microbes [3]. Literature studies disclosed that NAPs are establishing the antimicrobial propensity very adroitly and excellently countering to disease causing pathogens. The NAPs have distinct features [4,5] like very small size, their ability to pierce across the cell membrane easily, and their movement in whole parts of the body within short time make them dexterous substitute to conventional medicines [6,7]. Size, concentration and doping of different metals on NAPs (surface modification) are the significant features that predominantly improve their antimicrobial and antioxidant propensity [8-10]. Amongst NAPs, ZnO NAPs are very unique and distinguishing as they have imperious special optical, catalytic as well as electrochemical characteristics, high thermal stability, low operating properties, and high degree of transparency in visible region of spectrum [11]. Furthermore, due to wide band gap energy potential (3.6-3.8 eV), ZnO NAPs are

* Corresponding author: shakilchemist56@gmail.com

also considered among an important n-type semiconductor material [12]. Due to these remarkable characteristics they are being extensively engaged in several practical applications i.e. optoelectronic devices, Li-batteries, solid-state sensors as well as in solar cells [13-15]. ZnO, analogous to other semiconductor materials i.e. SnO_2, SiO_2 and TiO_2 which have wide band gap energy, express better and enhanced photo-catalytic propensities. ZnO NAPs doped with different metals have been superbly exploited for the photo-catalytic decomposition of several dyes as well as organic compounds [16]. But antioxidant as well as antimicrobial studies of un-doped and doped ZnO NAPs is being inspected till now [17] and their ability and efficiency towards them could be boosted by surface modification process (large surface area and grain size but small particle size). Surface modification can be accomplished by the doping phenomenon such as addition of dopant materials i.e. transition metals like (Mn, Fe, Cr, Sn, Co) and biomolecules at nanoscale level [11]. ZnO NAPs doped with transition metals and biomolecules; can be engaged as antimicrobial, biosensors, antioxidants, bio-imaging and drug delivery materials [12]. Cu is preferred for the doping purposes of ZnO NAPs rather than other transition metals because of the easily overlapping of its d-electrons with the ZnO valance bond [14]. This was examined that if Copper is doped on ZnO NAPs, then doped zinc oxide NAPs would be revealed improve and enhanced bioactivities [15] and magnetic propensities [16] that are suitable for spintronic and biomedicine applications [17-19]. As a result of doping, appreciation increase in the surface area and grain size but decreases in the particle size of ZnO NAPs would be taken place which will permit them to display improved and value-added antimicrobial and antioxidant potential [20]. So that's why, doping of Cu on ZnO NAPs is getting much more attention to attain surface modified NAPs with improved biological, magnetic and optical characteristics. Several methods are reported in literature for the synthesis of un-doped and doped NAPs but co-precipitation is considered to be as a simple, efficient, and cost effective method [20]. In the present research work, we successfully synthesized and developed the un-doped ZnO and Cu-doped ZnO NAPs through co-precipitation method. Optical and antibacterial properties were also evaluated for the fabricated NAPs.

2. Materials and Methods

2.1 Chemical reagents

The chemicals were procured from Merck (Germany). All the chemicals were of analytical grade. The chemicals such as ZnO (Zinc oxide), $Zn(NO_3)_2.6H_2O$ (Zinc nitrate hexahydrate), $Cu(NO_3)_2$ (Copper nitrate), $Cu(NO_3)_2.3H_2O$ (Copper nitrate trihydrate), Na_2CO_3 (Sodium carbonate) and sodium hydroxide (NaOH) were employed in this research work as a precursor. The other chemical and reagents were included nutrient agar, nutrient broth and methanol.

2.2 Bacterial strains

Human bacterial pathogens culture collections such as *Escherichia coli* (**ATCC** 25922) which cause different kinds of toxicities like urinary tract contaminations, food poisoning, neonatal meningitis and *Bacillus subtilis* (**ATCC** 9637), harvests several infections like sepsis, pneumonia and meningitis were obtained from PCSIR laboratories Lahore, Pakistan.

2.3 Synthesis of un-doped ZnO NAPs

The un-doped ZnO NAPs were manufactured through co-precipitation technique by employing $Zn(NO_3)_2.6H_2O$, Na_2CO_3 and NaOH as precursor constituents. The one molar zinc nitrate solution was prepared by dissolving the 14.427 g of $Zn(NO_3)_2.6H_2O$ in 50 ml of distilled water. The prepared zinc nitrate solution was subjected on magnetic stirrer at room temperature for one hr. A basic solution was prepared separately by dissolving four g of NaOH and 10.6 g of Na_2CO_3 in 50 ml of distilled water in order to maintain the pH value of the solution at 14. The basic solution was then added drop by drop to the initial solution under constant stirring and the reaction was allowed to proceed for 2 hr at room temperature to obtain white gel like precipitates. At the end of the reaction, the solution was placed intact and allowed to settle for overnight. The white precipitates were settled down at the bottom and the floating solution was discarded

carefully. The white precipitates were washed with distilled water several times until they became neutral. After washing, the final precipitates were placed in oven for drying at 120°C for 2 hr. After drying, the precipitates were ground in agate mortar. Finally, the collected NAPs were heated in a furnace at 500 °C for 2 hr.

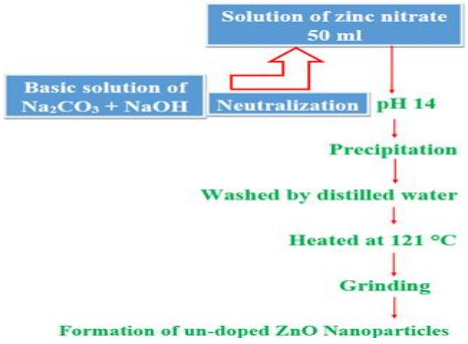

Fig. 1. Schematic diagram for the synthesis of un-doped ZnO NAPs

2.4. Synthesis of Cu-doped ZnO NAPs (M1 NAPs) through method 1

The 14.427 g of Zinc nitrate was dissolved in 50 ml of distilled water to prepare 1 M zinc nitrate solution. Then the solution was placed on magnetic stirrer under constant stirring at room temperature for 1 hr. 1 M solution of copper nitrate was prepared by dissolving 0.3624 g of copper nitrate in 50 ml of distilled water and then placed it under constant stirring at room temperature using a magnetic stirrer for 2 hr. The solutions of zinc nitrate and copper nitrate were mixed after complete dissolution. A basic solution was prepared separately by dissolving 4 g of sodium hydroxide and 10.6 g of sodium carbonate in 50 ml distilled water to maintain the pH value of the solution to 14. This basic solution was then added drop by drop to the combine solution of zinc nitrate and copper nitrate under constant stirring and this reaction was allowed to proceed for 2 hr at room temperature to obtain white gel like precipitates. At the end of the reaction, the solution was placed and allowed to settle for overnight. The white precipitates were settled down at the bottom and the floating solution on it was then thrown out carefully. The white precipitates were washed with distilled water several times until they became neutral. After washing, the final precipitates were placed in oven for drying at 120 °C for 2 hr. These dried precipitates were then ground in agate mortar. Finally, the collected nanoparticles were heated in a furnace at 500 °C for 2 hr.

Fig. 2. Schematic diagram for the synthesis of Cu-doped ZnO NAPs (M1 NAPs)

2.5 Synthesis of Cu-doped ZnO NAPs (M2 NAPs) through method 2

The copper doped ZnO NAPs were also prepared by using Zinc nitrate hexahydrate (Zn $(NO_3)_2.6H_2O$), copper nitrate trihydrate (Cu $(NO_3)_2.3H_2O$) and sodium hydroxide (NaOH) as starting materials. 1 M solution Zinc nitrate solution was prepared by dissolving 14.427 g of zinc

nitrate in 50 ml of distilled water. After that the solution was placed under constant stirring at room temperature using magnetic stirrer for 1 hr. Then, 1M solution of copper nitrate was prepared by dissolving 0.3624 g of copper nitrate in 50 ml distilled water and then placed it also under constant stirring at room temperature using a magnetic stirrer for 2 hr. Both the solutions of zinc nitrate and copper nitrate were mixed after stirring. Then, 1 M solution of sodium hydroxide was added drop wise to the combine solution of zinc nitrate and copper nitrate to adjust the pH value 14 of the solution. When the pH value reached to 14, this solution was allowed to settle for overnight. White, gelatinous precipitates were settled down at the bottom. Filtered these precipitates and washed with distilled water several times until they became neutral. Then, these precipitates were dried in an oven at 120 °C for 2 hr. After drying, these precipitates were ground in agate mortar. Finally, these nanoparticles were heated in a furnace at 200 °C for 3 hr.

Fig. 3. Schematic diagram for the synthesis of Cu-doped ZnO NAPs

2.6 Antibacterial activity

The antibacterial activity of the prepared un-doped ZnO and Cu-doped ZnO NAPs (M1 and M2 NAPs) was examined against two bacterial strains including both Gram positive (*Bacillus subtilis*) and Gram negative (*Escherichia coli*) bacteria which were obtained from PCSIR laboratories complex, Lahore, Pakistan. The antibacterial effect of un-doped ZnO NAPs and Cu-doped ZnO NAPs on agar plates was studied by employing agar diffusion method [21-25]. Cefradine was used as a positive control for both bacterial species and distilled water was used as a negative control against both species of bacteria i.e. *Bacillus subtilis* and *Escherichia coli.*

2.6.1 Agar well diffusion method

Sample solutions of four different concentrations were prepared in distilled water i.e. 1 M, 0.1 M, 0.25 M, 0.50 M and 0.75 M. Nutrient broth was prepared by taking 0.8 g of nutrient broth and dissolved it in 100 mL distilled water and then sterilized it in an autoclave and then cooled that solution. This medium used for the growth of the bacteria for the preparation of inoculum. The 1.6 g of nutrient broth was dissolved in 200 ml distilled water by applying heat. After that 2.6 g of nutrient agar was also added in it and heated it until a clear solution was obtained. Then it was sterilized in an autoclave at 121 °C for 15 minutes. Frozen bacteria were present in the stock slants of bacterial culture. That slants were taken and a loop full of culture or frozen bacteria was added to the sterilized nutrient broth in the test tube and preserved for future use. After that bacteria from stock slants were taken and added into two conical flasks in which nutrient agar was already added. These two cultures of two different bacteria were incubated at 37 °C for 24 hours in a shaker. These cultures used as inoculum. Freshly prepared molten nutrient agar (30 ml) was poured into the four sterilized petri dishes as a basal layer. After that 1mL inoculum of *E. coli* was added in two petri dishes and 1 ml inoculum of *B. subtilis* was added in remaining two petri dishes. Then put lids on the dishes and allowed them to cool and solidify. The solidify agar core 2 mm was bored at four peripheral positions by hollow iron rod. After that holes were filled with the four different concentrations of samples and reference standards. Then the petri dishes were allowed to place for 1 hr and after that incubated the dishes in incubator at 37 °C for 24 hrs in

order to complete the reaction for bioactivity. After the completion of incubation period the diameters of the clear zones were measured and recorded [26-29].

2.7 Statistical analysis

Statistical analysis has been applied on data through one-way or two-way ANOVA. Moreover, the Tukey post-test was also done employing Graph Pad Prism v6.04 software (Graph Pad Software, Inc., La Jolla, CA, USA). Differences between triplicates values were measured statistically at significant level of $p<0.05$. The figure legends are manifesting the group sizes. All values and data are communicated as their mean ± SD value.

3. Results

3.1 Characterization of fabricated un-doped ZnO and Cu-doped ZnO NAPs

Different analytical and spectroscopic techniques were employed to characterize the fabricated un-doped ZnO and Cu-doped ZnO NAPs (M1 NAPs and M2 NAPs). These techniques were XRD, SEM, EDX and UV-Vis spectroscopy. The XRD (PANalytical X'Pert Pro) gives the information about the characterization of the crystalline structure of the synthesized NAPs. The morphology of the prepared un-doped ZnO and Cu-doped ZnO NAPs was examined by SEM (Jeol, 5910LV). The EDX was employed to detect the number of elements as well as for the compositional analysis on the surface of the synthesized NAPs. UV-Vis spectroscopy studies provided the band gap energy of the un-doped ZnO and Cu-doped ZnO NAPs (M1 NAPs and M2 NAPs).

3.2 X-ray diffraction (XRD) studies

X-ray diffraction is a non-destructive analytical technique which provides the comprehensive statistics related to the crystallographic nature and chemical structure of synthetic as well as natural materials. XRD studies were performed on the fabricated un-doped ZnO and Cu-doped ZnO NAPs (M1 NAPs and M2 NAPs) to elaborate their size, shape as well as crystal structure and their results are depicted in the form of XRD spectra in Fig 4 (a), (b) and (c) respectively. The Fig. 4 (a) shows the typical XRD pattern of un-doped ZnO NAPs. The sharp diffraction peaks in the XRD pattern distinctly displays the crystalline nature of the manufactured un-doped ZnO NAPs and Cu-doped ZnO NAPs (M1 NAPs and M2 NAPs). But results indicated that un-doped ZnO NAPs is more in crystalline than Cu-doped ZnO NAPs as the contents of Cu rises, the intensity of XRD peaks declines and it displays the degradation of crystallinity (Fig 4). It means that the crystal defects around the dopants produced as a result of Cu doping in ZnO NAPs and the increase in charge imbalance resulting from this defect which lead toward changes in the materials stoichiometry and hence causing the crystallinity of materials to decrease [16]. Standard difffraction peaks represents the crystal structure of un-doped ZnO NAPs and Cu-doped ZnO NAPs (M1 NAPs and M2 NAPs) is hexagonal wurtzite structure according to the standard JCPDS data card. There are no diffraction peaks of other impurities detected which proves that the substance only belongs to the Zn. The average grain size of the synthesized un-doped ZnO NAPs was 15.63 nm which is calculated from the three most intense peaks (31.7, 34.35 and 36.15) using Debye-Scherer's formula. The Fig. 4 (b) displays the typical XRD patterns of synthesized Cu-doped ZnO NAPs with method 1 (M1 NAPs). The intense peaks show hexagonal wurzite structure of ZnO which is the most stable phase of ZnO. As seen in this XRD pattern below, there are no additional peaks correlates to Cu, CuO or Cu related phases and impurities. It may be due to the incorporation of Cu into the Zn lattice rather than interstitial spaces. The average grain size of the synthesized Cu-doped ZnO NAPs with method 1 (M1 NAPs) was 20.18 nm which is calculated from the three most intense peaks (28.25, 31.1, and 33.75) by means of Debye-Scherer's formula. The Fig. 4 (c) reveals the typical XRD pattern for the manufactured Cu-doped ZnO NAPs through method 2 (M2 NAPs). The intense peaks in this pattern also display the hexagonal wurzite structure of the ZnO. This graph shows no extra peaks corresponding to CuO or oxides of Cu or any other impurities related to copper. This also implies that Cu ion may be incorporated into the Zn lattice rather than interstitial sites. The average grain size of the synthesized Cu-doped ZnO

NAPs through method 2 (M2 NAPs) was 28.94 nm which is calculated from the three most intense peaks (31, 33.65 and 35.5) using Debye-Scherer's formula. Calculated grain size results indicated that the increase in grain size of the NAPs was perceived from 15.63 to 20.18 nm, then 20.18 nm to 28.94 nm. This increase in grain size of the fabricated Cu-doped ZnO NAPs was happened due to the effect of doping of Cu as the doping of transition metal accountable for the enhancement of the grain size of NAPs [27]. It also has been attributed that more level of Cu doping taken place in M2 NAPs rather than M1 NAPs as more increase in grain size observed in M2 NAPs than M1 NAPs. It has been reported that extent of increase in grain size of NAPs depends upon the level of the doping material on the surface of NAPs [29]. There is found a direct relation between the grain size and concentration of the dopants material. Our current findings found in close agreement with the previously reported data.

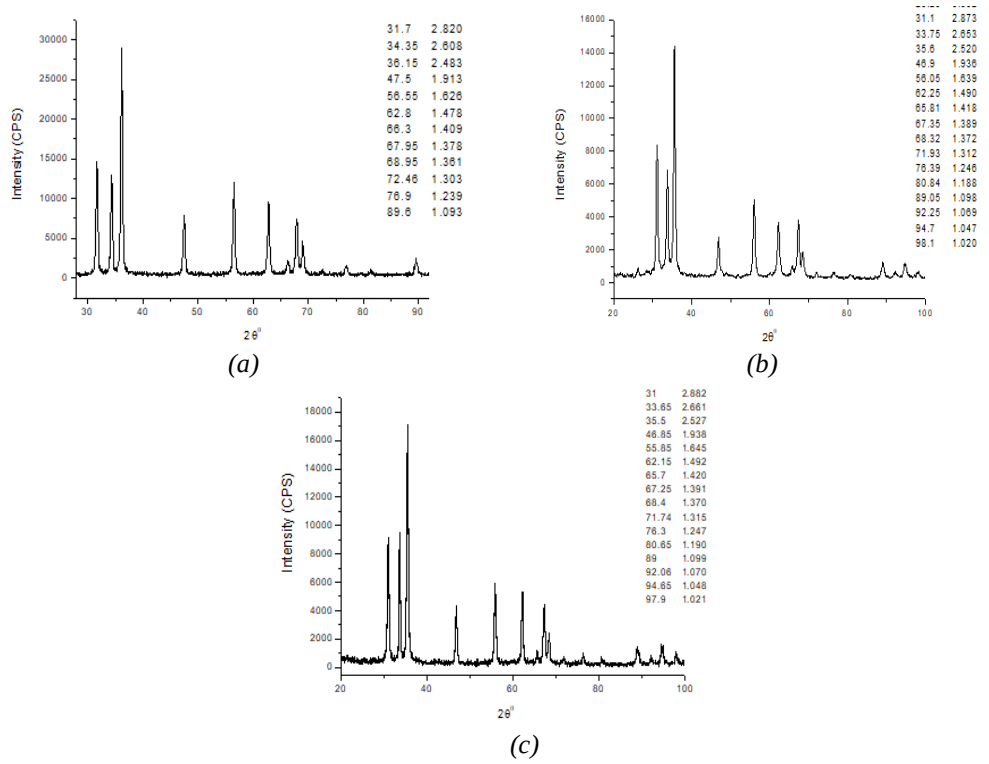

Fig. 4. XRD spectra for the synthesized un-doped ZnO NAPs (a), M1 NAPs (b) and M2 NAPs (c)

3.3 Scanning electron microscope studies

The structural characteristics and surface morphological analysis of manufactured un-doped ZnO and Cu-doped ZnO NAPs (M1 NAPs and M2 NAPs) were carried out through scanning electron microscopy (SEM) and the results of the each synthesized NAPs in the form of their SEM micrographs are presented in Fig. 5 (a), (b) and (c) respectively. SEM micrographs results were indicated and confirmed the grain size of the manufactured NAPs in nanometer range i.e. below 50 nm which is consistent with the results of XRD. SEM micrographs show that the synthesized un-doped ZnO NAPs are spherical in shape, equally distributed over the surface, homogeneous and crystalline in nature [Fig. 5 (a)]. However, the SEM results of the synthesized Cu-doped ZnO NAPs through method 1 (M1 NAPs) and method 2 (M2 NAPs) demonstrated that even though these NAPs are also equally distributed and homogenous in nature but less crystalline in contrast to un-doped ZnO NAPs while on the other hand M1 NAPs found to posses more crystallinity than M2 NAPs. The decrease in crystallinity was due to the fact of Cu doping that was accompanied more in M2 NAPs than M1 NAPs. Previous literature also elaborated and verdict of our SEM outcomes that doping of transition metal is the responsible factor to decrease the crystallinity of NAPs. There is found an inverse relationship between the crystallinity and doping. The shape of the synthesized Cu-doped ZnO NAPs through method 1 (M1 NAPs) and method 2

(M2 NAPs) is altered from the spheroid to rod like. The un-doped ZnO NAPs and M1 NAPs are not found well separated from each other but M2 NAPs observed to be separated (Fig 5). The SEM consequences illustrate that size and shape of the ZnO NAPs depends on the Cu additive. These results are in close agreement with the previous results [16,27].

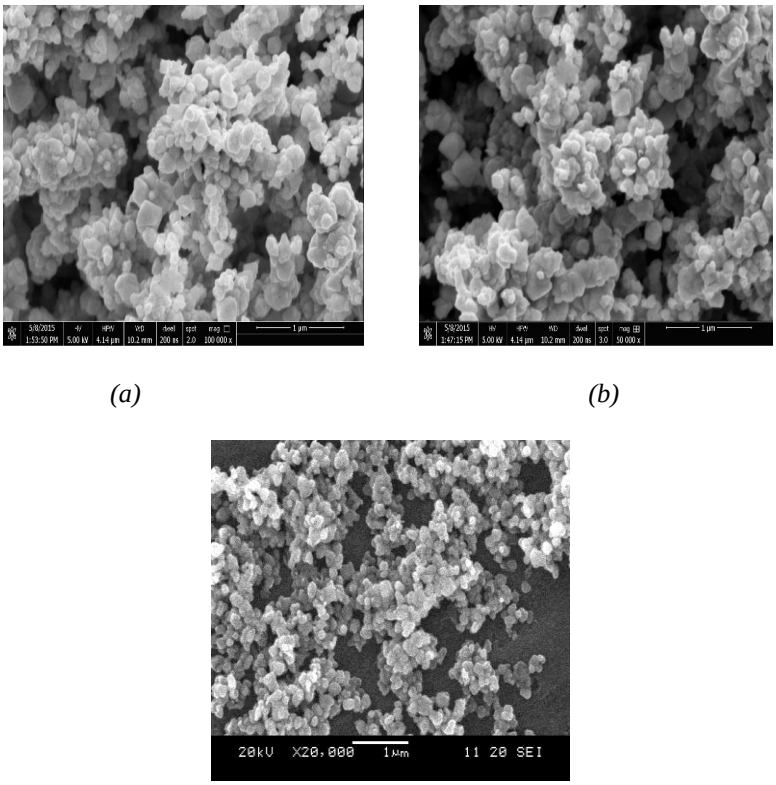

(a) *(b)*

(c)

Fig. 5. SEM micrographs for the synthesized un-doped ZnO NAPs (a), M1 NAPs (b) and M2 NAPs (c)

3.4 Energy-dispersive X-ray (EDX) spectroscopic analysis

The EDX was performed to examine the chemical composition and formation of the synthesized un-doped ZnO NAPs, Cu-doped ZnO NAPs through method 1 (M1 NAPs) as well as by method 2 (M2 NAPs). The results of EDX spectra for the fabricated un-doped ZnO NAPs, Cu-doped ZnO NAPs through method 1 (M1 NAPs) as well as by method 2 were predicted in Fig 6 (c), Fig 6 (a) and Fig 6 (b) respectively. The outcomes of the EDX spectra evidently validated the formation of un-doped and Cu-doped ZnO NAPs from both methods. Moreover, the EDX spectra affirmed the existence of chemical constituents (O-47.67%, Zn-52.31%) in un-doped ZnO NAPs while (O-46.67%, Cu-1.02 and Zn-52.31%) in M1 NAPs and (O-46.67%, Cu-5.02% and Zn-48.31%) in M2 NAPs. The peaks and chemical species associated with the impurities were not perceived in the EDX spectra which were found in consistent with XRD results. The sharp peaks of EDX spectra were revealed that the synthesized NAPs were crystalline in nature. EDX results were also elaborated that the ZnO diffraction peaks displayed strong intensity and narrow width which were vindicated that the resultant fabricated NAPs were highly crystalline in nature. EDX spectra were indicated that the more doping of Cu was perceived in M2 NAPs synthesized through method 2 than M1 NAPs which were synthesized through method 1 (Fig 6 a and b). Our current results of EDX were found in close proximity with the previous reports [16,27].

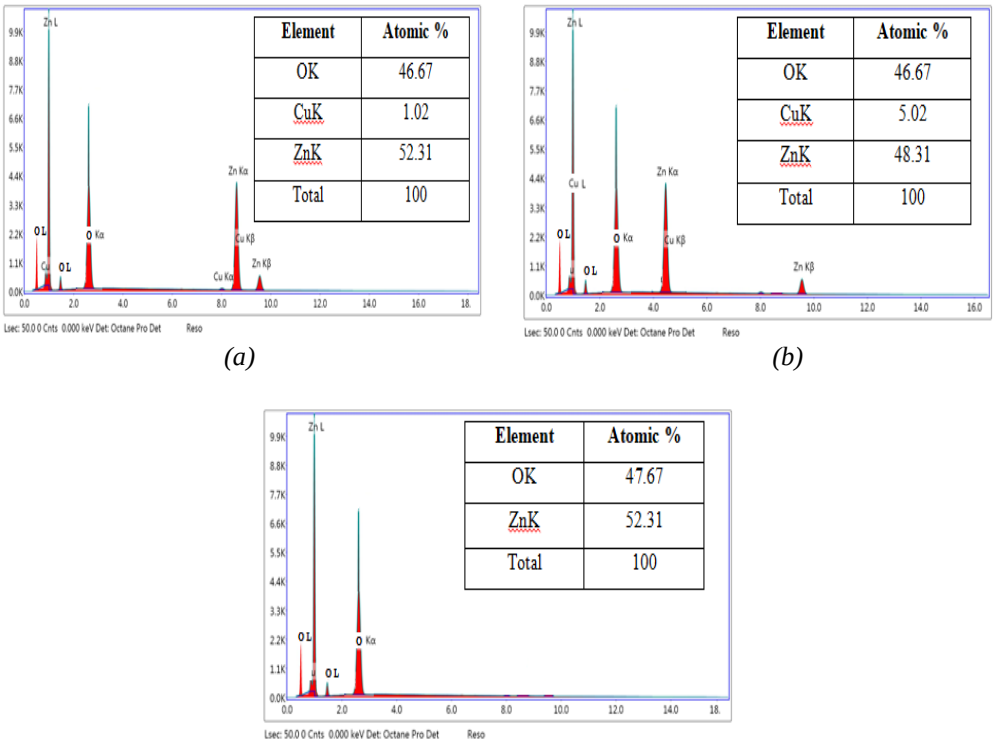

Fig. 6. EDX micrographs for the synthesized un-doped ZnO NAPs (c), M1 NAPs (a) and M2 NAPs (b)

3.5 UV-visible spectroscopy and band gap energy data

Band gap is defined as the difference in energy between the top valence bands and the bottom conduction band [16]. Band gap discloses the proficiency of electron to jump from one band to another. A definite minimum amount of energy is necessary for this transition from one band to another band [27]. The band gap energy data measurement executes an important role in semiconductors materials. For a material to be semiconductor, that material must have band gap energy of less than 3 eV and while for an insulator, it is greater than 4 eV which is larger than the band gap values of semiconductor materials [29]. Between linear fit and the photon energy axis, the value of Eg can be accomplished through the inter-section phenomenon. The d-electrons of Cu can easily over-lap with the valence band of ZnO as t2g levels (i.e. the dxy, dxz, and dyz orbitals are together pronounced as t2g levels). This is because of the fact that of t2g levels of copper is very close to valence bonds of ZnO [16]. The optical measurements of the synthesized NAPs have been executed to confirm the attribution of Cu^{+} substitution for Zn^{2+} by UV−vis−NIR spectroscopy at room temperature. The optical absorption spectra for the fabricated un-doped ZnO NAPs and Cu-doped ZnO NAPs (M1 NAPs and M2 NAPs) were shown in Fig 7. The un-doped ZnO NAPs exhibit a sharp absorption spectrum at 337 nm and they are manifesting the 3.68 eV band gap energy data at this absorption spectrum (337 nm) which contacts with the theoretical band gap Eg of ZnO. A fascinating outcome was perceived when 1.02 % and 5.02 % of Cu is inserting in the ZnO matrix (Cu-doped ZnO NAPs synthesized through method 1 and method 2) then the red shift of the Eg edge has been experimented from 3.68 to 2.76 and 2.10 eV and in terms of wavelength from 337 nm to 360 nm and 390 nm respectively (Fig 7). This fact of decreasing in energy band gap values was also previously professed in Mn and Cu-doped ZnO as well as in other transition metal doped oxides [29]. These verdicts can be explained on the basis of the exchange interactions of sp-d among localized d electrons of the Cu^{+} ions substituting Zn^{2+} ions and band electrons. The p-d and s-d exchange interactions result the positive and negative corrections to the valence band as well as conduction band edges, respectively, leading to a band-gap narrowing [27].

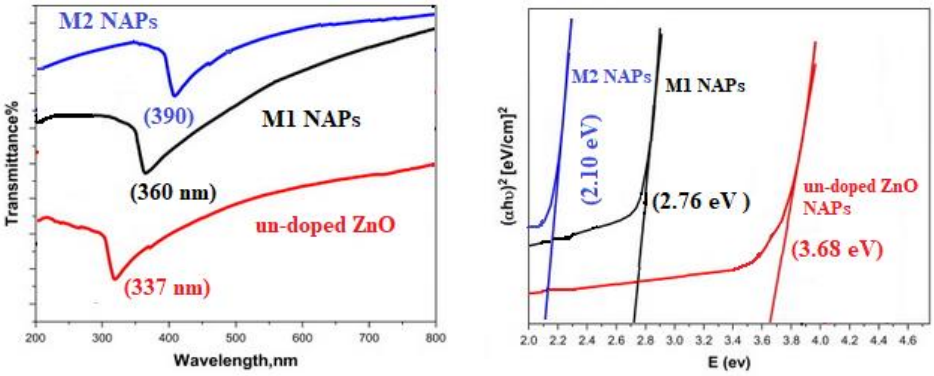

(a) *(b)*

Fig. 7. UV-visible spectra (a) and Band gap energy (b) of synthesized un-doped ZnO NAPs and Cu-doped ZnO NAPs (M1 NAPs and M2 NAPs)

3.6 Antibacterial activity

Bactericidal effects of synthesized un-doped ZnO NAPs and Cu-doped ZnO NAPs from method 1 (M1 NAPs) and method 2 (M2 NAPs) were studied against two different pathogenic bacteria i.e. *E. coli* and *B. subtilis.* These NAPs were dispersed in distilled water. Aqueous dispersions of un-doped ZnO NAPs and Cu-doped ZnO NAPs (M1 NAPs and M2 NAPs) of the desired concentrations were made; the effect of different concentrations (1 M, 0.75 M, 0.5 M, 0.25 M and 0.1 M) of un-doped ZnO NAPs and Cu-doped ZnO NAPs (M1 NAPs and M2 NAPs) against *E. coli* and *B. subtilis* was deliberated. The results of antibacterial propensity in the form of inhibition zone of dimeter (ZOIs) for the synthesized un-doped ZnO NAPs and Cu-doped ZnO NAPs (M1 NAPs and M2 NAPs) against *E. coli* and *B. subtilis* are presented in Fig. 8 (a) and Fig. 8 (b) respectively. Furthermore, the outcomes of minimum inhibitory concentration (MIC) and minimum bactericidal concentration (MBC) (mg/mL) are presented in Fig 9. The noteworthy and supreme antibacterial propensity against *E. coli* and *B. subtilis* was exhibited by the Cu-doped ZnO NAPs synthesized through method 2 (M2 NAPs) with all its concentration (0.1 M, 0.25 M, 0.50 M, 0.75 M and 1.0 M) in contrast to synthesized un-doped ZnO NAPs, Cu-doped ZnO NAPs synthesized from method 1 (M1 NAPs) and standard drug in the form of their MIC (23 ± 0.6, 19 ± 0.7 mg/mL) and MBC (32 ± 0.5, 22 ± 0.4 mg/mL) as well as ZOI values (Fig. 8 and 9) respectively. On the other hand, the Cu-doped ZnO NAPs synthesized through method 1 (M1 NAPs) with all its concentration (0.1 M, 0.25 M, 0.50 M, 0.75 M and 1.0 M) were revealed the improved and better antibacterial propensity against *E. coli* as well as *B. subtilis* than that of un-doped ZnO NAPs and standard drug (Cephradine) however the synthesized un-doped ZnO NAPs were corroborated the similar outcomes of antibacterial propensity as standard drugs were presented in this bioactivity as shown in Fig. 8 (a) and (b). The 1 M concentration of the synthesized M1 NAPs, M2 NAPs, un-doped ZnO NAPs and standard drug (Cephradine) was demonstrated the maximum antibacterial tendency in the form of their zone of inhibition values (27 ± 0.6 mm, 29 ± 0.8 mm, 31 ± 0.4 mm, 28 ± 0.3 mm) against *E. coli* in contrast to other concentrations (0.1 M, 0.25 M, 0.50 M and 0.75 M) respectively (Fig. 8 a). In the case of *B. subtilis*, maximum antibacterial bioactivity was also professed with the concentration of 1 M for the synthesized un-doped ZnO NAPs, M1 NAPs, M2 NAPs and standard drug (Fig. 8 b). Results validated and avowed that the antibacterial propensity of the synthesized NAPs was the function of doping of copper, and grain or crystallite size. Henceforth, results also exhibited the concentration dependent antibacterial propensity. Therefore, the synthesized Cu-doped ZnO NAPs (M1 NAPs and M2 NAPs) exposed greater and very effective broad spectrum antibacterial propensity than all other tested samples. But among Cu-doped ZnO NAPs, M2 NAPs vindicated the grater antibacterial activity than that of M1 NAPs as the more doping of Cu has been achieved through method 2 than method 1 [Fig. 6 (a) and (b)]. This was due to the fact of two reasons (i) more Copper doping that was achieved as seen in Figure 6 (b). (ii) Due to Cu doping, increase in grain size and surface area of these NAPs perceived [16] compared to un-doped ZnO NAPs (Fig. 4). As

more is the surface area and grain size with smaller particles size then more will be the antibacterial potential [27,29]. Henceforward, the synthesized M2 NAPs demonstrated very effective and significant broad spectrum antibacterial activities. Outcomes also revealed that the synthesized un-doped ZnO NAPs, Cu doped ZnO NAPs (M1 NAPs and M2 NAPs) as well as employed standard drug were found to display different antibacterial propensity against *E. coli* and *B. subtilis* in terms of ZOI, MIC and MBC. This is due to the fact of differences in chemical composition as well as structures of the cell surfaces as the cell wall of Gram negative bacteria (*E. coli*) is different from the Gram positive bacteria (*B. subtilis*) by having cover of the peptidoglycan layer outside the membrane [16,27].

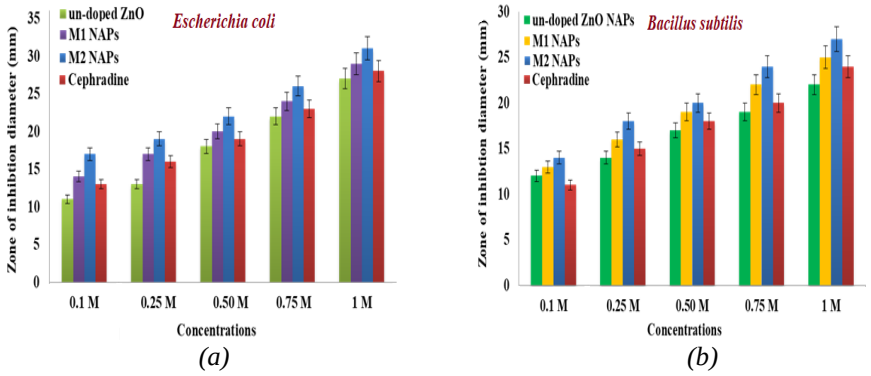

Fig. 8. ZOIs in antibacterial test of the synthesized un-doped ZnO NAPs, Cu-doped ZnO NAPs (M1 NAPs and M2 NAPs) and standard drug (Cephradine) against E. coli (a) and B. subtilis (b), (Values are mean ± SD triplicate assays)

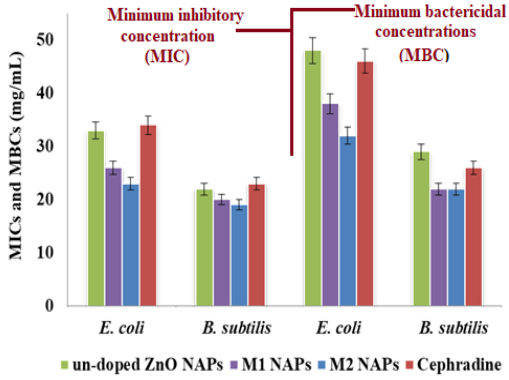

Fig. 9. Minimum inhibitory concentration (MIC) and minimum bactericidal concentration (MBC) of synthesized un-doped ZnO NAPs, Cu-doped ZnO NAPs (M1 NAPs and M2 NAPs) and standard drug (Cephradine) against E. coli and B. subtilis, (Values are mean ± SD triplicate assays).

4. Discussion

The un-doped ZnO NAPs and metal-doped ZnO NAPS have attained much attention by the researchers due to their important and domineering roles as a gas sensor, ceramic resistor, superconducting material, catalyst, as well as their roles in biological fields and in the energy sector [2,5]. The results of scanning electron microscope vindicated and affirmed the nano-range for the synthesized un-doped ZnO NAPs and Cu-doped ZnO NAPs synthesized through method 1 (M1 NAPs) and method 2 (M2 NAPs). The spherical shape of the synthesized un-doped ZnO NAPs and spheroid to Rod like shape for M1 NAPs and M2 NAPs were also affirmed from the results of SEM micrographs. Our current results of SEM are found in close agreement with the

previous reported studies [16]. Moreover, results obtained through EDX were found in consistent with the results of SEM. This was clearly manifesting from the spectrum results of EDX that the un-doped ZnO NAPs and Cu-doped ZnO NAPs (M1 NAPs and M2 NAPs) were manufactured magnificently. The EDX spectra results disclosed that the major components of the synthesized NAPs were of Zn, O, and Cu; no impurities were perceived as the peaks linked to impure chemical components were absent in the EDX spectra of each synthesized NAPs. The strong, intense, narrow width and sharp peaks in the EDX spectrum were justified that the fabricated NAPs (un-doped and doped NAPs) were crystalline in nature. EDX results were exhibited that the doping of copper was observed in M2 NAPs synthesized through method 2 than M1 NAPs synthesized through method 1. The results of EDX in the existing study are comparable to previously reported data [27]. The sharp peaks of the synthesized un-doped ZnO NAPs and Cu-doped ZnO NAPs synthesized through method 1 (M1 NAPs) and method 2 (M2 NAPs) were perceived in the XRD spectrum, which established their crystalline nature and supported the EDX results. The calculated grain size through the most intense peaks of the XRD spectrum was 15.63 nm, 20.18 nm, and 28.94 nm for the un-doped ZnO NAPs, M1 NAPs and M2 NAPs respectively. This increase in grain size was resulted due to the incorporation of Cu as dopant materials on the surface of ZnO matrix which leads to the increase in grain size. There is found a direct relationship between the grain size and the concentration of dopant material. The un-doped ZnO NAPs exhibit a sharp absorption spectrum at 337 nm and they are manifesting the 3.68 eV band gap energy data at this absorption spectrum (337 nm) which contacts with the theoretical band gap Eg of ZnO. A fascinating outcome was perceived when 1.02 % and 5.02 % of Cu is inserting in the ZnO matrix (Cu-doped ZnO NAPs synthesized through method 1 (M1 NAPs) and method 2 (M2 NAPs) then the red shift of the Eg edge has been experimented from 3.68 to 2.76 and 2.10 eV and in terms of wavelength from 337 nm to 360 nm and 390 nm respectively (Fig 7) [16]. This decrease in bad gap values and increase in wavelength (Red shift) of the synthesized Cu-doped ZnO NAPs (M1 NAPs and M2 NAPs) was resulted due to the doping of copper as previous results are also corroborated the same effect of metal doping on the band gap as well as wavelength. More the metal doping on the matrix of un-doped NAPs, decrease in band gap values might be taken place. Our current results of optical band gap and UV-Visible studies found in close proximity with the previous reported data [29]. Hence the results of XRD, SEM, EDX, and UV-Visible spectroscopic analysis are found to support the outcomes of each other.

The Cu-doped ZnO NAPs synthesized through method 1 (M1 NAPs) at the concentration of 1 M fashioned greater bactericidal effects than the un-doped ZnO NAPs and standard drug Cephradine in the growth inhibition of *E. coli* and *Bacillus subtilis*. While Cu-doped ZnO NAPs synthesized through method 2 (M2 NAPs) demonstrated the strong and superior bacteriological effect in contrast to standard drug, M2 NAPs and un-doped ZnO NAPs through deterring the growth of *E. coli*, as well as *B. subtilis*. This greater and significant bactericidal activity was because of the fact that more doping of Cu has been achieved through method 2 which leads to increase in grain size (surface modification process). Large surface area and grain size is the responsible factor to exhibit extraordinary antibacterial activity by the M2 NAPs. The antibacterial effect increases with increasing concentration of NAPs. This study affirms the use of un-doped and doped metal NAPs as future antibacterial agents. The proposed mechanism for the bactericidal activity of the synthesized Cu-doped ZnO NAPs is shown in Fig. 10. So the more number of copper ions released from Cu-doped ZnO NAPs pervaded through the bacterial cell membrane and demolished the cell membrane structure by attaching to the negatively charged cell wall through the electrostatic interactions [16].

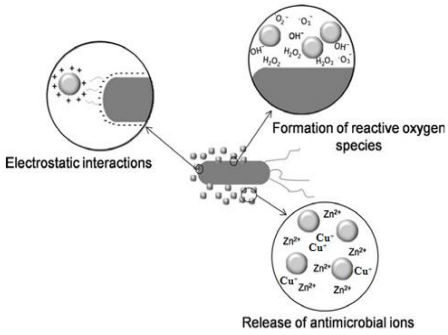

Fig. 10. Proposed mechanism for the action of Cu-doped ZnO NAPs to demolish bacterial cell

As result of electrostatic interaction between the NAPs and the surface of bacterial strains produced reactive oxygen species (ROS) on the surface of cell wall which leads to the cell damage due to oxidative stress on the cell wall. Moreover, zinc ions as well as Cu^{+} ions are involved in cross linkage of nucleic acid strands by binding them with DNA molecule of bacteria. This results in a disordered helical structure of DNA molecule which causes denaturation of proteins and some other biochemical processes in the cell, leading to complete destruction of the bacterial cell [27]. Factors which affect the sensitivity of bacteria to Cu-doped ZnO NAPs are the size of particles, the temperature of synthesis of the nanoparticles, structure of bacterial cell wall, and degree of contact of the nanoparticles with bacteria [29].

5. Conclusions

In the current research study, optical and antibacterial properties of un-doped ZnO NAPs and Cu-doped ZnO NAPs were evaluated. The optical studies verdict that the Cu-doped ZnO NAPs synthesized from method 2 (M2 NAPs) posses less energy band gap values than M1 NAPs and un-doped ZnO NAPs and hence M2 NAPs exhibit their features and characteristics more towards semiconductors. The results of this study also designate that the synthesized un-doped ZnO NAPs and Cu-doped ZnO NAPs synthesized from method 1 (M1 NAPs) and method 2 (M2 NAPs) have effective and anticipated biological properties as Cu-doped ZnO NAPs (M2 NAPs) disclosed improved and extraordinary broad spectrum bactericidal results against gram negative bacterial (*E. coli*) as well as gram positive bacterial (*B. subtilis*) in contrast to employed standard drugs, M1 NAPs and un-doped ZnO NAPs. This was due to the fact of physical features of the Cu-doped ZnO NAPs (M2 NAPs) i.e. large surface with increase grain size and smaller particle size. Our current work also elaborated that the method 2 for the synthesis of NAPs is more appropriate than method 1 as more doing was experimented with method 2. Consequently, these synthesized NAPs hold enormous potential for use in the cosmetic, nutraceutical and pharmaceutical industries.

Acknowledgement

This work was supported by the Department of Chemistry, School of Science, University of Management and Technology, Lahore, Pakistan.

References

[1] S.P. Gubin, Magnetic nanoparticles. Wiley-VCH 2009; ISBN 3-527-40790-1.
[2] K. M. Reddy, K. Feris, J. Bell, D. G. Wingett, C. Hamley, A. Punnoose, Applied Physics Letter **90**, 2139021 (2007).

[3] A. Anukaliani, G. Manjula, M. Nair, M. Nirmala, K. Rekha, Material Letter **65**, 1797 (2011).
[4] Y. Wang, X. Zhao, L. Duan, F. Wand, H. Niu, W. Guo, A. Ali, Material Science Semiconductor Process **29**, 372 (2015).
[5] S. Chawla, S.K. Jayanthi, Applied Surface Science **257**, 2935 (2011).
[6] M. Hoffman, S. Martin, W. Choi, D. Behnemann, Chemical Reviews **95**, 69 (1995).
[7] B. Straumal, B. Baretzky, A. Mazilkin, S. Protasava. Journal of European Ceramic Society **29**, 1963 (2009).
[8] K. H. Tam, A. B. Djurisic, C. M. N. Chan, Y. Y. Xi, C. W. Tse, Y.H Leung, W. K. Chan, F.C.C. Leung, D.W.T. Au, Thin Solid Film **516**(18), 6167 (2008).
[9] W. Göpel, K.D. Schierbaum, Sensor and Actuator B-Chem **26**(1-3), 1 (1995).
[10] S. A. Khan, S. Shahid, F. Ijaz, Green Synthesis of Copper Oxide Nanoparticles & Biomedical Application, Publisher: Lambert Academic Publishing, ISBN: 978-620-2-02718-2 1, 1-133 (2017).
[11] S. Shahid, S.A. Khan, W. Ahmad, U. Fatima, S. Knawal, Indian Journal of Pharmaceutical Sciences 80(1), 173 (2018).
[12] K. Anandan, V. Rajendran, Journal of Non-Oxide Glasses **2**, 83 (2010).
[13] S.A. Khan, S. Shahid, W. Bashir, S. Kanwal, A. Iqbal, Tropical Journal of Pharmaceutical Research **16**(10), 2331 (2017).
[14] A. Dodd, A. McKinley, M. Saunders, T. Tsuzuki, Nanotechnology **17**(3), 692 (2006).
[15] K. Dutta, S.K. De, Material Letter **61**(27), 4967 (2007).
[16] S.A. Khan, F. Noreen, S. Kanwal, G. Hussain, Digest Journal of Nanomaterials and Biostructures, **12**(3), 877 (2017).
[17] S.A. Khan, S. Shahid, S. Kanwal, G. Husaain, Dyes and Pigments **148**(C), 31 (2017).
[18] G. Hussain, S.A. Khan, W. Ahmad, M. Athar, R. Saleem, International Journal of Advanced Research **5**(4), 234 (2017).
[19] S.A. Khan, S. Shahid, M. Jameel, A. Ahmad, International Journal of Pharmaceutical Chemistry **6**(4), 107 (2016).
[20] F. Ijaz, S. Shahid, S.A. Khan, W. Ahmad, S. Zaman, Tropical Journal of Pharmaceutical Research **16**(4), 743 (2017).
[21] S.A. Khan, S. Shahid, W. Ahmad, S. Ullah, International Journal of Pharmaceutical Science and Research **2**(2), 22 (2017).
[22] W. Ahmad, S.A. Khan, K.S. Munawar, A. Khalid, S. Kawanl, Tropical Journal of Pharmaceutical Research **16**(5), 1137 (2017).
[23] S.A. Khan, S. Shahid, M.R. Sajid, F. Noreen, S. Kanwal, International Journal of Advanced Research **5**(6), 925 (2017).
[24] S.A. Khan, M. Jameel, S. Kanwal, S. Shahid, International Journal of Pharmaceutical Science and Research **2**(3), 29 (2017).
[25] S.A. Khan, N. Rasool, M. Riaz, R. Nadeem, U. Rashid, K. Rizwan, M. Zubair, I.H. Bukhari, T. Gulzar, Asian Journal of Chemistry **25**(13), 7457 (2013).
[26] S.A. Khan, S. Shahid, Z.A. Khan, A. Iqbal, International Journal of Scientific Research and Publications **6**(3), 529 (2016).
[27] S.A. Khan, F. Noreen, S. Kanwal, A. Iqbal, G. Hussain, Materials Science and Engineering: C **82**C, 46 (2018).
[28] S.A. Khan, S. Kanwal, A. Iqbal, W. Ahmad, International Journal of Advanced Research, **5**(4), 1350 (2017).
[29] M. A. Qamar, S. Shahid, S. A. Khan, S. Zaman, M. N. Sarwar, Digest Journal of Nanomaterials and Biostructures, **12**(4), 1027 (2017).